Let us continue the discussion of octahedral ligand filed. We begin with the cartesian coordinate expression of the potential.

$$v_{\text{cb}}(\boldsymbol{r}) = eD \left(x^4 + y^4 + z^4 - \frac{3}{5}r^4. \right) \tag{2.68}$$

In eq. (2.1), the above potential should be $\mathcal{H}_{\text{CF}}$, which now has more priority than $\mathcal{H}_{\text{SOI}}$ for present. First we consider the single-electron problem in the central force plus octahedral potential. Since our problem is on the $3d$ electrons in an open shell, we restrict ourselves to the space generated on the basis of d-orbital wavefunctions. Also it can be known from the group theory, that will be introduced afterwards, the potential in (2.68) does not split s and p orbitals, as can be easily guessed by considering the symmetry of $p_{x,y,z}$.

In order to diagonalize this potential within d-orbitals ($l = 2$) ϕ_{nlm}: $(n, l, m) = (n, 2, m = 2, 1, 0, -1, -2)$, in an orthodox way, we write down the secular equation and then obtain the eigenvalues and the eigenvectors[1]. But here, we deduce the functional forms of diagonalization basis functions from a simpler thought[2]. The radial part is common for d-orbitals (rather for principal quantum number n). The parts of spherical harmonic functions are

$$Y_{20}(\theta, \varphi) = \sqrt{\frac{5}{16\pi}}(3\cos^2\theta - 1), \tag{2.69a}$$

$$Y_{2\pm1}(\theta, \varphi) = \mp\sqrt{\frac{15}{8\pi}}\cos\theta\sin\theta e^{\pm i\varphi}, \tag{2.69b}$$

$$Y_{2\pm2}(\theta, \varphi) = \sqrt{\frac{15}{32\pi}}\sin^2\theta e^{\pm 2i\varphi}. \tag{2.69c}$$

This directional dependences in cartesian coordinate are quadratic in (x, y, z) as $r\cos\theta = z$, $r\sin\theta\cos\varphi = x$, $r\sin\theta\sin\varphi = y$. Since the non-spherical part in the potential (2.68) is given as an even function of (x, y, z), off-diagonal elements of the matrix representation on the (partial) basis of the quadratic functions yz, zx, xy are zero by integrating out the odd functions. Residual quadratics are x^2, y^2, z^2. For vanishing off-diagonal terms in the matrix representation for $x^4 + y^4 + z^4$, we need to take differences between (x^2, y^2, z^2). Possible independent candidates are $x^2 - z^2$, $y^2 - z^2$ though they are not orthogonal. Hence with orthogonalization we reach $3z^2 - r^2$, $x^2 - y^2$.

These directional dependencies can be obtained in the linear combination of eq. (2.69) as

$$\phi_\xi = \frac{i}{\sqrt{2}}(\phi_{n21} + \phi_{n2-1}) = \sqrt{\frac{15}{4\pi}}\frac{yz}{r^2}R_{n2}(r), \tag{2.70a}$$
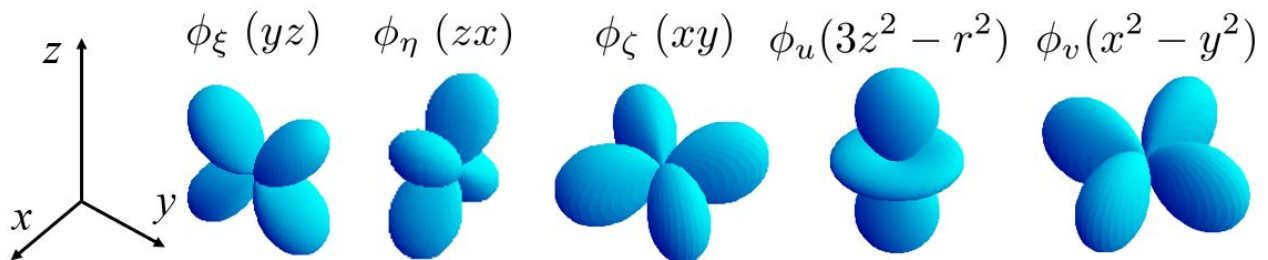
Fig. 2.9 Eigenstates of d-electron in an octahedral ligand field (eq. (2.70)). The surfaces of (absolute value of wavefunction)=(constant) are drawn with shading.
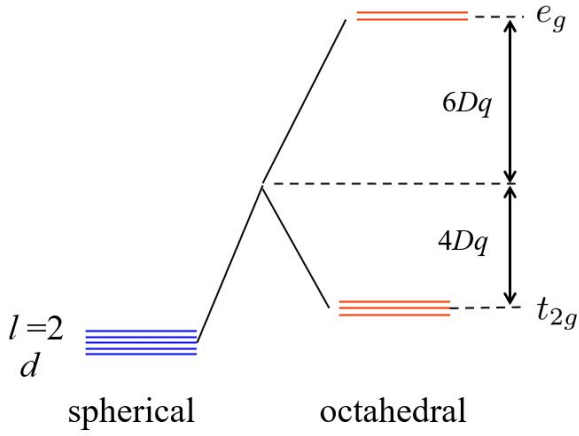
Fig. 2.10 Level splitting of d-orbital by an octahedral ligand potential. D, q are defined in eq. (2.67) and eq. (2.71) respectively. The uniform increase of levels by the constant term is also drawn.

$$\phi_\eta = -\frac{1}{\sqrt{2}}(\phi_{n21} - \phi_{n2-1}) = \sqrt{\frac{15}{4\pi}}\frac{zx}{r^2}R_{n2}(r), \tag{2.70b}$$

$$\phi_\zeta = -\frac{i}{\sqrt{2}}(\phi_{n22} - \phi_{n2-2}) = \sqrt{\frac{15}{4\pi}}\frac{xy}{r^2}R_{n2}(r). \tag{2.70c}$$

And

$$\phi_u = \phi_{320} = \sqrt{\frac{5}{16\pi}}\frac{3z^2 - r^2}{r^2}R_{n2}(r), \tag{2.70d}$$

$$\phi_v = -\frac{1}{\sqrt{2}}(\phi_{322} + \phi_{32-2}) = \sqrt{\frac{5}{16\pi}}\frac{x^2 - y^2}{r^2}R_{n2}(r). \tag{2.70e}$$

The "shapes" of these wavefunctions are expressed in Fig. 2.9 as shaded surfaces of (absolute value of direction-dependent part in the wavefunction)=(a constant).

We restrict ourselves to $3d$ electrons. Let q be

$$q = \frac{2e}{105}\langle r^4\rangle = \frac{2e}{105}\int |R_{32}(r)|^2 r^4(r^2 dr), \tag{2.71}$$

and the group of three wavefunctions ϕ_ξ, ϕ_η, ϕ_ζ and the group of two wavefunctions ϕ_u, ϕ_v have the eigen energies

$$\epsilon_1 = -4Dq, \quad \epsilon_2 = 6Dq \tag{2.72}$$

respectively. The states corresponding to ϵ_1 and ϵ_2 are called T_{2g}, E_g respectively named after the point groups. The single-electron orbitals belonging to those are called t_{2g} (or $d\epsilon$) orbital and e_g (or $d\gamma$) orbital. The level splitting of d-orbital is illustrated in Fig. 2.10. The shift between t_{2g} and e_g is roughly explained from the shapes of wavefunctions drawn in Fig. 2.9 as follows. The three orbitals of t_{2g} have zero amplitude when one of (x, y, z) is zero, avoiding the positions of ligands, hence decrease the Coulomb energy. On the other hand, e_g orbitals elongate to the directions of ligand, enhancing the Coulomb energy.

The angular moments of these orbitals are zero. For example, $\langle\phi_\zeta|l_z|\phi_\zeta\rangle$ gets +2 from ϕ_{322}, -2 from ϕ_{32-2}, and the total is zero. Similarly $\langle\mathbf{l}^2\rangle = 0$. This is the result of linear combination, in which the sum of the orbital angular momentum vanishes. In other words, the eigenstates are the standing waves for the octahedral potential, naturally have zero angular momentum. Very important conclusion of this analysis is that the result explains the experimental results in Tab. 2.4, in which the effective number of Bohr magneton appears to be as if the orbital angular moment vanishes.

2.7.2 Ground states of multiple electrons

Next we should consider the electron configuration in these t_{2g}, e_g orbitals along with the Hund's rule. Here we need to compare the crystal (ligand) field splitting $10Dq$ and the energy gain of the exchange integral (eq. (2.20c)) by following
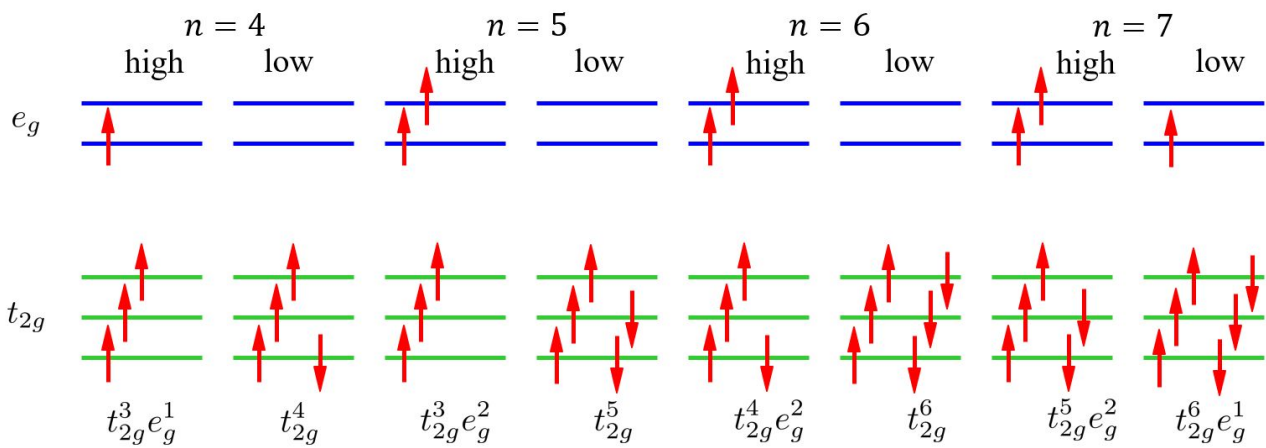
Fig. 2.11   Two possible electron accommodations of t_{2g} and e_g orbitals. There are high-spin states and low-spin states for electron numbers more than $n = 4$.

the Hund's rule. When the former surpasses the latter, the configuration of more accommodation in t_{2g} orbital with lower total spin is favored. Such a multiple-electron state is called low-spin state.

Figure 2.11 shows possible spin configurations (high- and low-spin states) for $n = 4 \sim 7$. For $n = 8, 9$, t_{2g} orbitals are fully occupied, and there is a single possible configuration. In the example of an iron ion Fe^{2+} in a hemoglobin, the existence of two possible (high, low) spin states brings about a dramatic effect. Four nitrogen atoms of porphyrin and imidazole nitrogen at the end of the globin protein polypeptide chain are coordinated to this iron ion, which is not a regular octahedron coordination. However we still take t_{2g}, e_g orbitals as the basis since the splitting due to the further lowering in the symmetry is not very large. When the complex structure does not have an oxygen atom, namely a five coordination state, the electrons are in a high-spin state ($t_{2g}^4 e_g^2$) while under the coordination of an oxygen atom (one of two in a molecule), the splitting $10Dq$ between t_{2g}-e_g becomes larger and the state transits to the low-spin state t_{2g}^6. The transition can be detected by, e.g., the electron spin resonance.
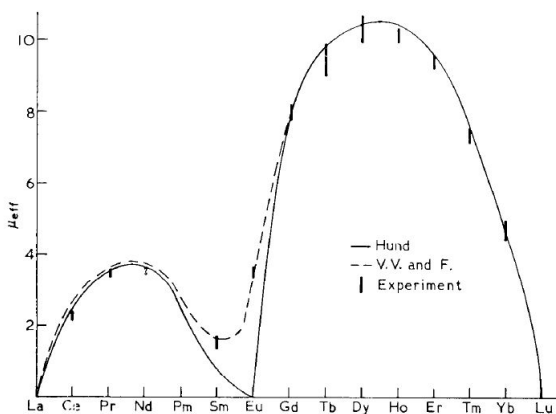
The ground state of t_{2g} or e_g still has 3-fold or 2-fold degeneracy. When the octahedral structure gets a distortion along z-axis, the degeneracy is lifted and generally the energy of ground state lowered. Hence when the energy lowering of the ground state surpasses the energy increase due to the lattice distortion, the lattice-distorted state is favored and the symmetry lowered. This phenomenon is called the **Jahn-Teller effect** and observed, e.g., in $CuSiF_6 6H_2O$ salt. Or in some cases, the crystal field effect is coupled to the lattice vibration yielding the effect called dynamic or vibronic Jahn-Teller effect.

2.7.3   Van Vleck paramagnetism

In the above, on the paramagnetism of $3d$ transition metals and $4f$ lanthanoid, we have seen that, the former can be understood by considering the effect of ligand field while the latter can be fairly understood by considering the SOI via LS coupling (or j-j coupling) approach. However we still have a problem in the latter. As we see in Tab. 2.5, there are big discrepancies between the theory and the experiment for Eu^{3+}, Sm^{3+}. The problem was theoretically solved by Van Vleck, and the phenomenon is called Van Vleck paramagnetism. The above figure is from the Nobel lecture[3] given by

Van Vleck, which demonstrates that his theory quantitatively explains the discrepancies in the simple theory.

Let us see how the theory works in the case of Eu^{3+}. The electron configuration is $4f^6$, the electron number is less than $2l + 1 = 7$, then we see the coefficient of $\boldsymbol{L} \cdot \boldsymbol{S}$ is positive from eq. (2.38). Namely $\boldsymbol{L}$ and $\boldsymbol{S}$ couple as anti-parallel. The ground state is $^7F_0$, which means $J = 0$. In the excited states, possible total angular momenta are $J = 1, 2, \cdots, 6$. From eqs. (2.38),(2.41),

$$\mathcal{H}_{\mathrm{SOI}} = \lambda \boldsymbol{L} \cdot \boldsymbol{S} = \frac{\lambda}{2}[J(J+1) - S(S+1) - L(L+1)]. \tag{2.73}$$

The splitting width of LS-multiplet (L, S are fixed, J is the index of split states) is

$$\Delta E_{LS} = E_{LS}(J) - E_{LS}(J-1) = \lambda J. \tag{2.74}$$

The energy difference between the ground state with $J = 0$ and the first excited state with $J - 1$ is λ, which is as small as $200 \sim 300$ K. Hence even at low temperatures, when there is a finite external magnetic field, the term $\mathcal{H}_{\mathrm{SOI}}$ causes mixing of the state $J = 1$ with the $J = 0$ ground state, which gives rise to a finite magnetic moment.

2.8   Symmetry and degeneracy of quantum states

In the above we have solved a specific problem of d-electrons in an octahedral potential. In more general treatment, we should apply regular perturbation theory. However, the thoughts from the symmetry of the system is very helpful in the calculation since we can largely decrease the amount of calculation[4]. The symmetry of a system is defined by **symmetry operations**. A symmetry operation is a transformation in a space of some degrees of freedom. Examples are rotations, parallel transformations, mirror reflections, etc. in the coordinate space. When a system is invariant under a symmetry operation, the system has the symmetry for the operation. The total symmetry of a system is defined as a set of symmetries possessed by the system. In the following we will have a short look at a general method to know the degeneracy of quantum states from the symmetry of the system.

2.8.1   Symmetry operations in point groups

We use **group** theory for such discussions. In Appendix 3A, we have seen that symmetry operations constitute a group, an element of which has a corresponding matrix of representation. Thus the symmetry of a system can be specified by the corresponding group. The symmetry groups that have correspondence to spatially localized systems are called **point groups**. Particularly in crystals, the constraint of discrete translational symmetry restricts the number of possible point groups called "crystal point groups" to 32 listed in Tab. 2.6.

We won't go deep into mathematics though the group theoretical knowledges of symmetry operation are indispensable for the researchers of crystallography, symmetry-sensitive properties like multi-ferroics. Embarrassing in symmetry group theories is that similar symbols are

The problem with handling a group of symmetric operations is that they are all confusing with similar symbols to various concepts, and the symbols are different and more confusing depending on the style of the mathematicians. In physics, Schönflies and Mulliken symbols have been used, and we also follow that here but recently "international standard" symbols are also frequently used. At present I cannot find the way to describe the expressions in a beautifully organized manner.

When a set of functions $\mathscr{A}_\varphi = \{\varphi_1, \varphi_2, \cdots\}$ is transformed back to itself by a symmetry operation R, that is, $\mathscr{A} \xrightarrow{R} \mathscr{A}'_\varphi = \{\varphi'_1, \varphi'_2, \cdots\} = \mathscr{A}$, $\mathscr{A}$ can be a representation basis of R and the corresponding matrix is given as

$$D_{ij}(R) = \langle \varphi_i | R | \varphi_j \rangle. \tag{2.75}$$

system	Schönflies symbol	Hermann-Mauguin symbol		examples
		full	abbreviated	
triclinic	C_1	1	1	
	$C_i, (S_2)$	$\bar{1}$	$\bar{1}$	Al_2SiO_5
monoclinic	$C_{1h}, (S_1)$	m	m	KNO_2
	C_2	2	2	
	C_{2h}	2/m	2/m	
orthorhombic	C_{2v}	$2mm$	mm	
	$D_2, (V)$	222	222	
	$D_{2h}, (V_h)$	2/m2/m2/m	mmm	I, Ga
tetragonal	C_4	4	4	
	S_4	4	4	
	C_{4h}	4/m	4/m	$CaWO_4$
	$D_{2d}, (V_d)$	$\bar{4}2m$	$\bar{4}2m$	
	C_{4v}	$4mm$	$4mm$	
	D_4	422	42	
	D_{4h}	4/m2/m2/m	4/mmm	TiO_2, In, β-Sn
rhombohedral	C_3	3	3	AsI_3
	$C_3, (S_6)$	3	3	$FeTiO_3$
	C_{3v}	$3m$	$3m$	
	D_3	32	32	Se
	D_{3d}	32/m	$3m$	Bi, As, Sb, Al_2O_3
hexagonal	$C_{3h}, (S_3)$	6	6	
	C_6	6	6	
	C_{6h}	6/m	6/m	
	D_{3h}	62m	62m	
	C_{6v}	$6mm$	$6mm$	ZnO, NiAs
	D_6	622	62	CeF_3
	D_{6h}	6/m2/m2/m	6/mmm	Mg, Zn, graphite
cubic	T	23	23	$NaClO_3$
	T_h	2/m3	$m3$	FeS_2
	T_d	43m	43m	ZnS
	O	432	43	β-Mn
	O_h	4/m32/m	$m3m$	NaCl, diamond, Cu
icosahedral	C_5	5	5	
	$C_{5i}, (S_{10})$	10	10	
	C_{5v}	$5m$	$5m$	
	C_{5h}, S_5	5	5	
	D_5	52	52	
	D_{5d}	52/m	5/m	C_{80}
	D_{5h}	$1\bar{0}2/m$	$1\bar{0}2/m$	C_{70}
	I	532	532	
	I_h			C_{60}

Tab. 2.6 Crystal systems, Schönflies symbols, Hermann-Mauguin symbols and examples of materials of 32 crystal point groups. From Ref. [4].

	Symmetry operation	Rotation axis	Number of operation
E	Identical transformation		1
C_4	$\pi/2$ rotation around 4-fold axis	x, y, z	3
$C_2 = C_4^2$	π rotation around 4-fold axis	x, y, z	3
C_4^3	$3\pi/2$ rotation around 4-fold axis	x, y, z	3
C_2	π rotation around 2-fold axis	(0,1,1), (1,0,1), (1,1,0)	6
		(0,1,−1), (−1,0,1), (1,−1,0)	
C_3	$2\pi/3$ rotation around 3-fold axis	(1,1,1), (1,1,−1), (1,−1,1), (−1,1,1)	4
C_3^2	$4\pi/3$ rotation around 3-fold axis	(1,1,1), (1,1,−1), (1,−1,1), (−1,1,1)	4

Tab. 2.7 Symmetry operations octahedral group (O group).

Here, if $D(R)$ can get further block diagonalization by unitary matrix S (i.e., replacement of basis) as

$$SD(R)S^{-1} = \begin{pmatrix} D_1(R) & & 0 \\ & D_2(R) & \\ 0 & & \ddots \end{pmatrix}, \tag{2.76}$$

$D(R)$ is **reducible** and can be expressed as a **direct summation** of $D_1(R), D_2(R), \cdots$ as

$$D(R) = D_1(R) \oplus D_2(R) \oplus \cdots . \tag{2.77}$$

On the other hand, if such block diagonalization is impossible, the representation is **irreducible**. Expression of a reducible representation as a direct summation of irreducible representations, is called reduction.

Irreducible or reducible namely the possibility of block diagonalization cannot be judged from the simple diagonalizability of matrix. Often adopted is the use of **character** table. Character of representation is the trace of representation matrix, which is invariant for the changing of basis. Hence a character for reducible representation is the sum of characters for irreducible representations in the direct summation. From this the reduced form in the direct summation can be deduced.

Table 2.7 lists the symmetry operations that keep an octahedral system invariant. Those operations constitute a group called octahedral group, of which the symbol is O. As in Tab. 2.6, it belongs to the cubic symmetry. The octahedral complex systems with magnetic ions also have the space-inversion symmetry in addition to O. Hence to be strict, we need to consider O_h group. Although here for simplicity we consider O group and it is known that the level-splitting behavior is the same for O_h. Group O has 24 symmetry operations as the elements as listed in this table.

	O	E	$8C_3$	$3C_2 = 3C_4^2$	$6C_2'$	$6C_4$
$\Gamma_{l=0}$	A_1	1	1	1	1	1
$\Gamma_{l=1}$	T_1	3	0	−1	−1	1
$\Gamma_{l=2}$	$E + T_2$	5	−1	1	1	−1
$\Gamma_{l=3}$	$A_2 + T_1 + T_2$	7	1	−1	−1	−1
$\Gamma_{l=4}$	$A_1 + E + T_1 + T_2$	9	0	1	1	1
$\Gamma_{l=5}$	$E + 2T_1 + T_2$	11	−1	−1	−1	1
Γ_1	A_1	1	1	1	1	1
Γ_2	A_2	1	1	1	−1	−1
Γ_{12}	E	2	−1	2	0	0
Γ_{15}'	T_1	3	0	−1	−1	1
Γ_{25}'	T_2	3	0	−1	1	−1

Tab. 2.8 Symmetry operations in group O (topmost low), and characters. The representations in the upper low are on bases of eigenfunctions of orbital angular momentum. Those in the lower low display irreducible representations.

Next we consider the representations of these symmetry operations. A simple choice of representation basis is the eigenfunctions in a system of a spherical potential. They can have the orbital angular momentum as the quantum number, namely $s, p, d, f, \cdots$. The representations based on them are listed in the upper band in Tab. 2.8. The symbols $\Gamma_{l=0} \sim \Gamma_{l=5}$ are the representations on the orbital angular momentum l. However they are not generally irreducible. The symbols of irreducible representations are named in the following way. A, E, T are for 1, 2, and 3-dimensional representations. The suffices do not have strict rule, being numbered starting from O group. In the table, the irreducible representations A_1, A_2, E, T_1, T_2 of group O and the characters are listed in the lower band. From the comparison of these characters, we know that $\Gamma_{l=0}, \Gamma_{l=1}$ are irreducible. This fact indicates that s and p orbitals do not split in an octahedral potential. For $l \geq 2$, Γ_l are reduced as indicated in the table. When we consider the split of d-orbital, we added suffix g as T_{2g} and E_g. Actually we need to consider group O_h including the space-inversion operation i. The symmetry operations are the direct product with i and the number of i operations brings the difference between even number (gerade, g in Germany) and odd number (ungerade, u). The irreducible representation also needs the suffix of g (even).

2.8.2 Symmetry operation and degeneracy

Let R be one of such symmetry operation and a function φ transform as

$$\varphi' = R\varphi. \tag{2.78}$$

Assume an operator $\mathcal{O}$ is transformed by R to $\mathcal{O}'$, then the operation of $\mathcal{O}'$ on the transformed function $R\varphi$ should be the result of operation R on the $\mathcal{O}$-operated original φ. Therefore

$$\mathcal{O}'R\varphi = R\mathcal{O}\varphi = R\mathcal{O}R^{-1}R\varphi.$$

That is, $\mathcal{O}$ is transformed to $R\mathcal{O}R^{-1}$. Now assume $\mathcal{H}$ is invariant for the symmetry operation R.

$$R\mathcal{H}R^{-1} = \mathcal{H}, \quad \therefore [R, \mathcal{H}] = 0. \tag{2.79}$$

Let ϕ an eigenfunction of $\mathcal{H}$ with an eigenvalue of E, that is $\mathcal{H}\phi = E\phi$. Then

$$\mathcal{H}R\phi = R\mathcal{H}R^{-1}R\phi = RE\phi = ER\phi, \tag{2.80}$$

which indicates that $\phi' = R\phi$ is an eigenstate of $\mathcal{H}$ with the same eigenvalue E. If ϕ and ϕ' are independent to each other, they are degenerate eigenfunctions. This degeneracy is based on the symmetry of the system. Other kinds of degeneracy is called "accidental" and usually lifted by some factors in real systems.
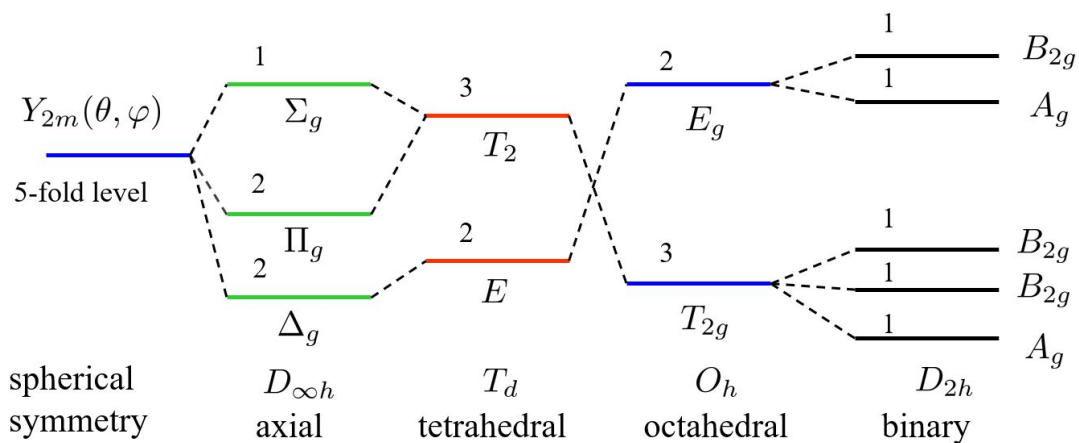
Fig. 2.12 Level splitting of 5-fold $l = 2$ states in various symmetries expressed by crystal point groups. The numbers attached to the levels indicate the degree of degeneracy. From Ref. [4].

Let $\{\phi_i\}$ be eigenfunctions with degree of degeneracy d with eigenvalue E of $\mathscr{H}$. The representation matrix of R in this space is given by

$$D_{ij}(R) = \langle \phi_i | R | \phi_j \rangle. \tag{2.81}$$

That is,

$$R\phi_\nu = \sum_{\mu=1}^{d} D_{\mu\nu}(R)\phi_\mu. \tag{2.82}$$

Here $D(R)$ must be irreducible. Otherwise, e.g., assume $D(R)$ is block diagonalized as

$$D(R) = D_1(R) \oplus D_2(R) = \begin{pmatrix} D_1(R) & 0 \\ 0 & D_2(R) \end{pmatrix}.$$

Then the basis is transformed by the transformation matrix for the reduction as $\{\phi_i\} \rightarrow \{\chi_i\}$. We can thus divide the basis $\{\phi_i\}$ into $\{\phi_i^{(1)}\}$ and $\{\phi_i^{(2)}\}$ which belong to $D_1(R)$ and $D_2(R)$ respectively. They are not transformed to each other by symmetry operation, hence the degeneracy is accidental.

From the above discussion and by the character tables of irreducible representation, we can deduce how the degenerate states under consideration split when the symmetry of the system changes. Further we can know the shape of wavefunction from the basis of representation, hence infer the order of energy levels. Thus obtained level splitting of d-orbitals in various ligand field potentials is illustrated in Fig. 2.12.

2.9 Experiments and applications of localized spins

We have studied magnetic atoms or ions, which have large localized magnetic moments based on the measurement of magnetic susceptibility and the crystal structures. Here we have a look at fundamentals of magnetic resonance – a very important experimental method for magnetism. As an application of paramagnetic salt, we have short visit to magnetic refrigeration.

2.9.1 Magnetic resonance

In Sec. 2.1.2, we have mentioned that the magnetic moment tilted in a static magnetic field causes Larmor precession. In the method of **magnetic resonance** (MR), by applying an oscillating magnetic field at the Larmor frequency and by observing the resonance, we obtain not only the information of the magnetic moment itself, but also that of the environment surrounding the moment. It is needless to say the academic and social importance.

Let $\boldsymbol{J}$ be the total angular momentum of an isolated electron system. The Zeeman term in a static magnetic field $\boldsymbol{B}_0$ along z axis is given by

$$\mathcal{H}_1 = g_J \mu_{\mathrm{B}} \boldsymbol{J} \cdot \boldsymbol{B}_0, \tag{2.47}$$

which is just the same as eq. (2.47). Heisenberg equation of motion is written as

$$\frac{d\boldsymbol{J}}{dt} = \frac{i}{\hbar}[g_J \mu_{\mathrm{B}} \boldsymbol{J} \cdot \boldsymbol{B}_0, \boldsymbol{J}], \tag{2.83}$$
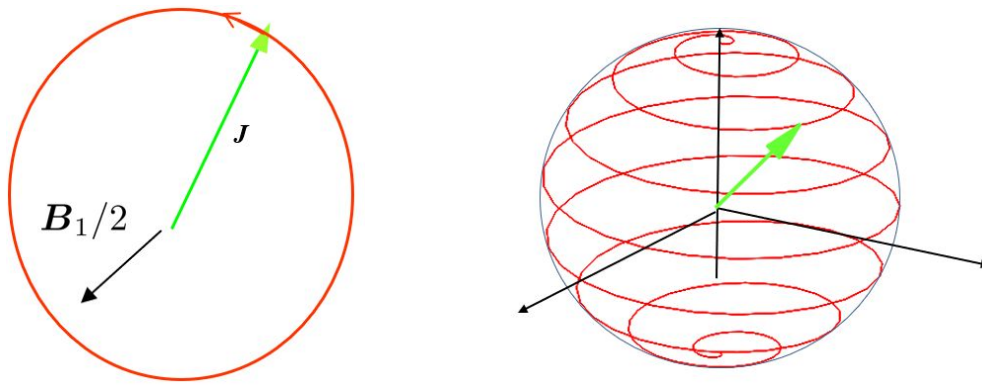
to which the commutation relation

$$J_y J_z - J_z J_y = iJ_x, \quad J_z J_x - J_x J_z = iJ_y, \quad J_x J_y - J_y J_x = iJ_z \tag{2.84}$$

is applied to obtain

$$\frac{d\boldsymbol{J}}{dt} = \frac{g_J \mu_{\mathrm{B}}}{\hbar} \boldsymbol{B}_0 \times \boldsymbol{J}. \tag{2.85}$$

Fig. 2.13 Left: Precession of angular momentum $\boldsymbol{J}$ around the in-plane magnetic field $\boldsymbol{B}_1/2$ on the rotating coordinate. Right: Illustration of the total motion tracing the end-point of $\boldsymbol{J}$ from the static coordinate. Under realistic conditions, the rotation around z-axis is much faster.

This expresses the precession with Larmor frequency

$$\omega_{\mathrm{L}} = g_J \frac{eB_0}{2m}. \tag{2.86}$$

Now if we observe this precession from the coordinate rotating around z-axis with frequency ω_{L}, the precession is canceled out and the momentum looks as if it sits still. Namely in this coordinate, the effect of static field along z axis vanishes and virtually zero-field state is realized.

An oscillation magnetic field $\boldsymbol{B}(t) = \boldsymbol{B}_1 \cos(\omega t)$ (on the non-rotating coordinate) perpendicular to the static field $\boldsymbol{B}_0$ can be written as the sum of rotating field as

$$\boldsymbol{B}(t) = \frac{\boldsymbol{B}_1}{2}[\exp(i\omega t) + \exp(-i\omega t)]. \tag{2.87}$$

When $\omega \approx \omega_{\mathrm{L}}$, from the rotating coordinate the ω-component almost sits still while the $-\omega$-component is rotating with 2ω. We take **rotating wave approximation**, in which the latter is ignored. Now on the rotating coordinate, a static field of $B_1/2$ is applied in xy-plane and the angular momentum starts precession around this field with frequency

$$\omega_1 = g_J \frac{eB_1}{4m}. \tag{2.88}$$

This is the basic process of **magnetic resonance**.

Figure 2.13 illustrates the motion of angular momentum under a magnetic resonance, in which the end-point draws a spiral. Note that under realistic conditions, the rotation around z-axis is much faster.

References

[1] C.J. Ballhausen. *Introduction to Ligand Field Theory (Advanced Chemistry)*. McGraw-Hill Inc.,US, 12 1962.

[2] Joachim Stöhr and Hans Christoph Siegmann. *Magnetism: From Fundamentals to Nanoscale Dynamics (Springer Series in Solid-State Sciences, 152)*. Springer, 9 2006.

[3] J. H. Van Vleck. Quantum mechanics: The key to understanding magnetism. *Science*, Vol. 201, No. 4351, pp. 113–120, July 1978.

[4] Mildred S. S. Dresselhaus. *Group Theory: Application to the Physics of Condensed Matter*. Springer, 10 2010.